

Probing the alignment of ultracold spin-polarized Rb₂ molecules

Markus Deiß, Björn Drews, Benjamin Deissler, and Johannes Hecker Denschlag

Institut für Quantenmaterie and Center for Integrated Quantum Science and Technology IQST, Universität Ulm, 89069 Ulm, Germany

(Dated: December 3, 2024)

We demonstrate a method to probe the alignment of the molecular axis of spin-polarized ultracold dimers. Diatomic ⁸⁷Rb₂ molecules are held in the lowest Bloch band of a far-off resonance 3D optical lattice. Using lattice modulation spectroscopy we measure the molecular polarizabilities, which are directly linked to the alignment, along each of the *x*-, *y*-, and *z*-directions of the lab coordinate system. In contrast to nonrotating molecules, we observe that rotating molecules have an anisotropic orientation of the molecular axis. Furthermore, we derive the dynamical polarizabilities for a laser wavelength of 1064.5 nm parallel and orthogonal to the molecular axis of the dimer, $\alpha_{\parallel} = 8.9(9) \times 10^3$ a.u. and $\alpha_{\perp} = 0.9(4) \times 10^3$ a.u., respectively.

PACS numbers: 33.15.Kr, 33.15.Bh, 37.10.Pq, 67.85.-d

For many applications in molecular physics and chemistry, control over orientation and alignment of the molecular axis in the laboratory frame is essential [1, 2]. For instance, in stereochemistry, chemical reaction rates are studied depending on the orientation and the movement of molecules [3–5]. Moreover, alignment is important for diffractive imaging of molecules [6–9], photodissociation [10–12], surface reactions [13, 14], as well as ultrafast molecular physics [15, 16]. To achieve molecular alignment, various methods have been proposed and demonstrated, including collisional alignment [17, 18], “brute force” methods using strong dc electric or magnetic fields [19–21], alignment using strong ac pulsed fields [1, 22, 23], or combinations of ac and dc fields [11, 24–26]. Most of these schemes rely on an external field to align the molecular axis. This leads to the hybridization of the field-free rotational states into so-called pendular states in the presence of an interaction potential which depends on the angle between the molecular axis and the field. An alternative way to create sizable alignment is to prepare a spin-polarized sample of molecules in specific rotational eigenstates. In contrast to other methods, no strong fields are required for this method. The alignment persists as long as a quantization axis is defined, and is efficient since all polarized molecules participate.

Experiments with ultracold molecules open up a wide range of prospects due to the extraordinary control over all degrees of freedom, including the preparation of well-defined rotational and spin-polarized states [27]. In terms of orienting cold molecules, first experiments were performed in 2011 in which polar KRb molecules were exposed to a dc electric field [28]. Afterwards, the anisotropic polarizability of these polar molecules was demonstrated in a 1D optical lattice of which the polarization was rotated [29]. Very recently, rovibrational states with specific alignment have been identified in experiments with Rydberg molecules [30].

In this Letter, we report on measurements of the alignment of ultracold nonpolar ⁸⁷Rb₂ molecules in the vibrational ground state of the $a^3\Sigma_u^+$ potential. The molecules are associated from two spin-polarized atoms and are trapped in the lowest Bloch band of a 3D optical lattice. By modulating the lattice potential in an appropriate way we measure the polarizability of the molecules for all three directions in space. From

these data we can infer the alignment of the molecular axis with respect to the lattice axes.

When a nonpolar molecule is exposed to a linearly polarized, oscillating electrical field $\vec{E}(t) = \hat{\epsilon}E_0\cos(\omega t)$ with amplitude E_0 and unit polarization vector $\hat{\epsilon}$, a dipole potential $U = -\hat{\epsilon} \cdot (\vec{\alpha}\hat{\epsilon})E_0^2/4$ is induced. Here, $\vec{\alpha}$ is the polarizability tensor, which is in general frequency dependent. In a molecule-fixed coordinate system, the polarizability tensor of a diatomic molecule is diagonal and its components have two values, α_{\parallel} and α_{\perp} , for the directions parallel and perpendicular to the molecular axis. U can then be written as $U = -(\alpha_{\parallel}E_{\parallel}^2 + \alpha_{\perp}E_{\perp}^2)/4$ where E_{\parallel} and E_{\perp} are the corresponding components of the electric field amplitude. We describe the orientation of the molecular axis by a unit vector $\vec{A} = (A_x, A_y, A_z) = (\sin\theta\cos\phi, \sin\theta\sin\phi, \cos\theta)$, where θ (ϕ) denotes the polar (azimuthal) angle, see Fig. 1(a). Using $E_{\parallel}^2 = (\hat{\epsilon} \cdot \vec{A})^2 E_0^2$ and $E_{\perp}^2 = E_0^2 - E_{\parallel}^2$ the potential becomes $U = -[\alpha_{\parallel}(\hat{\epsilon} \cdot \vec{A})^2 + \alpha_{\perp}(1 - (\hat{\epsilon} \cdot \vec{A})^2)]E_0^2/4$. In a quantum mechanical treatment $(\hat{\epsilon} \cdot \vec{A})^2$ is replaced by its expectation value $\langle(\hat{\epsilon} \cdot \vec{A})^2\rangle$. Using electric fields with amplitudes $E_{0,i}$ and polarizations $\hat{\epsilon}_i$ that point in each of the directions ($i = x, y, z$) of the lab coordinate system we measure the molecular polarizabilities $\alpha^{(i)} = 4|U_i|/E_{0,i}^2$, where

$$\alpha^{(i)} = \langle A_i^2 \rangle \alpha_{\parallel} + (1 - \langle A_i^2 \rangle) \alpha_{\perp}. \quad (1)$$

The quantity $\langle A_i^2 \rangle$ (or more generally $\langle(\hat{\epsilon} \cdot \vec{A})^2\rangle$) defines the degree of molecular alignment with respect to the direction $\hat{\epsilon}_i$ (or $\hat{\epsilon}$). For nonaligned molecules, all $\langle A_i^2 \rangle$ are equal to 1/3. Clearly, by measuring the polarizability $\alpha^{(i)}$ we can directly determine $\langle A_i^2 \rangle$ once α_{\parallel} and α_{\perp} are known.

For the $a^3\Sigma_u^+$ state the dynamics of the molecular axis are well described by that of a quantum rotor, where the Hamiltonian is essentially given by \vec{R}^2 , and \vec{R} is the operator for molecular rotation (see for example [31]). Thus, for the purpose of our investigation, we ignore coupling of \vec{R} to any other spins or angular momenta [32]. Consequently, R is a good quantum number and the eigenstates of the axial motion are the spherical harmonics $Y_{R,m_R}(\theta, \phi) \equiv |R, m_R\rangle$. Here, m_R is the projection of R onto the quantization axis in the *z*-direction.

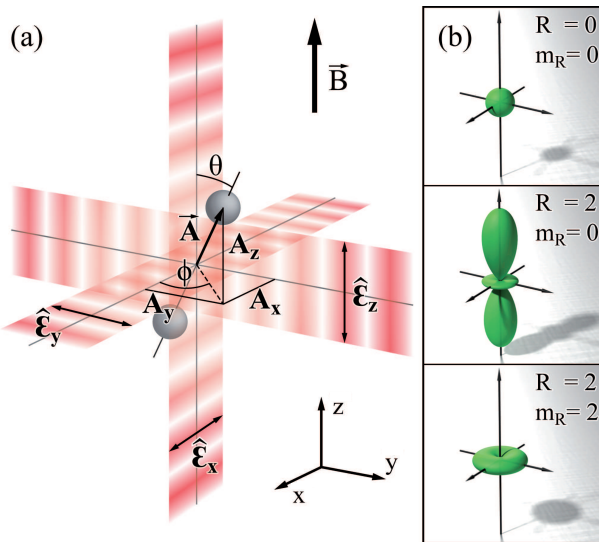


FIG. 1. (Color online). (a) Schematic of the experiment. Three laser beams with linear polarizations $\hat{\epsilon}_x$, $\hat{\epsilon}_y$ and $\hat{\epsilon}_z$ orthogonal to each other form a 3D optical lattice. The molecular axis of a diatomic molecule is given by \vec{A} . The magnetic field \vec{B} points in the z -direction and represents the quantization axis. (b) Polar plots of $|Y_{R,m_R}(\theta, \phi)|^2$ for the three accessible states $|R, m_R\rangle = |0, 0\rangle, |2, 0\rangle, |2, 2\rangle$.

The degree of alignment of the molecular axis with respect to the x -, y -, and z -directions can be calculated as

$$\langle A_i^2 \rangle = \int |Y_{R,m_R}|^2 A_i^2 \sin(\theta) d\theta d\phi. \quad (2)$$

Figure 1(b) shows the polar plots of $|Y_{R,m_R}|^2$ for the three relevant rotational quantum states in our experiments. For $|R=0, m_R=0\rangle$ the axis direction is isotropic in space, indicating a nonaligned molecule. In contrast, the axis direction is anisotropic for $|2,0\rangle$ and $|2,2\rangle$, which is directly reflected in degrees of molecular alignment different from $1/3$.

Our experimental setup and the molecule preparation has been described in detail in refs. [33, 34]. In brief, a BEC or ultracold thermal ensemble of spin-polarized ^{87}Rb atoms ($f_a = 1$, $m_{f,a} = 1$) is loaded into a 3D optical lattice, in which Feshbach molecules are associated at a magnetic field of $B = 1007.4\text{ G}$. After a purification step and an optical STIRAP transfer (stimulated Raman adiabatic passage) at $B = 1000\text{ G}$ to the vibrational ground state of the $a^3\Sigma_u^+$ potential, we obtain a pure ensemble of 1.5×10^4 molecules. By changing the relative detuning of the STIRAP lasers we can choose to populate either of the rotational levels $|R, m_R\rangle = |0, 0\rangle$ or $|2, 0\rangle$, which are separated by about 1.9 GHz (see [31]). Both molecular states have quantum numbers $m_F = 2$, $f = 2$, $I = 3$ and $S = 1$, where m_F is the projection of the total angular momentum F onto the quantization axis and f denotes the total angular momentum without molecular rotation \vec{R} . I and S are the total nuclear and electronic spin quantum numbers. The molecules reside within the lowest Bloch band of the optical lattice with no more than a single molecule per lattice site. The optical lattice consists of a superposition of three linearly polarized

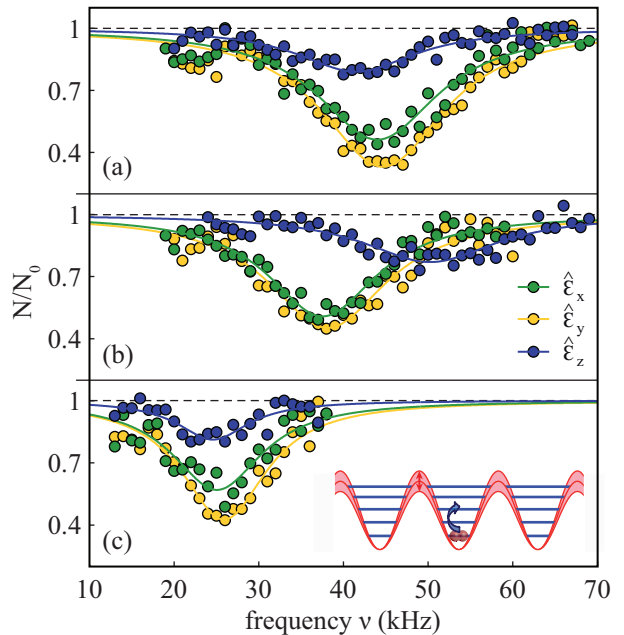


FIG. 2. (Color online). Amplitude modulation spectroscopy. The general scheme is sketched in the inset in (c) illustrating the resonant modulation of the lattice depth in one direction. The data show resonances for molecules in states $|0, 0\rangle$ (a) and $|2, 0\rangle$ (b), as well as for Feshbach molecules (c) at $B = 1000\text{ G}$. We measured the fraction of remaining molecules, N/N_0 , as a function of the modulation frequency ν for the three different lattice directions. Here, $\hat{\epsilon}_x$, $\hat{\epsilon}_y$ and $\hat{\epsilon}_z$ indicate the electric field of which the amplitude has been modulated (cf. Fig. 1(a)). Each data point of an excitation spectrum is the average of between 5 and 25 repetitions of the experiment (for a given molecular state and direction i the number of repetitions is constant). The statistical error of each data point is typically in the range of $\pm(0.05 - 0.15)$. Solid lines correspond to Lorentzian fits.

standing light waves in the x -, y -, and z -directions with polarizations orthogonal to each other, see Fig. 1(a). Each lattice beam has a wavelength of $\lambda = 1064.5\text{ nm}$, a linewidth of a few kHz and relative intensity fluctuations of less than 10^{-3} . In order to avoid interference effects, the frequencies of the standing waves are offset by about 100 MHz relative to each other. At the location of the atomic sample, the waists ($1/e^2$ -radii) of the lattice beams are about $130\text{ }\mu\text{m}$ and the maximum available power per beam is about 3.5 W .

We now independently determine the three molecular polarizabilities, $\alpha^{(i)}$ ($i = x, y, z$), which, according to Eq. (1), are directly linked to the degrees of molecular alignment $\langle A_i^2 \rangle$. Since $\alpha^{(i)} = 4|U_i|/E_{0,i}^2$, we need a measurement of both the lattice depth U_i and the field amplitude $E_{0,i}$. In order to measure U_i we consider the lattice beam with polarization $\hat{\epsilon}_i$ in the direction i (see Fig. 1). We use amplitude modulation spectroscopy [35, 36] in which the amplitude of this lattice beam is sinusoidally modulated over 10 modulation periods. A resonant modulation frequency drives transitions from the lowest Bloch band to the second excited band (see inset in Fig. 2(c)) giving rise to losses. At the end of each experimental cycle, the fraction N/N_0 of molecules remaining is measured. For

this purpose, the atom signal is detected via absorption imaging after reversing the STIRAP and dissociating the Feshbach molecules. By comparing the resonant transition frequency to a band-structure calculation of the sinusoidal lattice, the lattice depth U is determined.

Figure 2 shows excitation spectra after amplitude modulation for vibrational ground state molecules in states $|0,0\rangle$ and $|2,0\rangle$ as well as for weakly bound Feshbach molecules at a magnetic field of $B = 1000$ G. For each measurement, we determine the center of the excitation resonance using a Lorentzian fit. Due to technical reasons the modulation strength varied between the three lattice directions (6% peak-peak intensity modulation in case of the electric field pointing in x -direction, 5% in y -direction and 2% in z -direction), leading to different depths of the resonances. We have checked that the variation in modulation strength does not affect the resonance positions. We observe that for nonrotating molecules in $|0,0\rangle$ (Fig. 2(a)), the resonant excitation frequencies in the three different modulation directions are very similar, whereas in case of $|2,0\rangle$ (Fig. 2(b)), the lattice depth for $\hat{\epsilon}_z$ -polarization is much higher than for the other two polarizations, indicating an alignment of molecules along the z -direction.

In order to determine the electric field amplitudes $E_{0,i}$ we perform the lattice modulation measurements with weakly bound Feshbach molecules for the same experimental parameters as for deeply bound molecules (Fig. 2(c)). In this way, the polarizability can be determined independently of the exact beam parameters. We use $\alpha_{\text{Rb+Rb}}^{(i)} = 4|U_i|/E_{0,i}^2$ and the fact that the polarizability of weakly bound Feshbach molecules, $\alpha_{\text{Rb+Rb}}$, is isotropic and known to be twice the atomic polarizability $\alpha_{\text{Rb}} = 693.5(9)$ a.u. [37]. Here, 1 a.u. = $4\pi\epsilon_0 a_0^3 = 1.649 \times 10^{-41} \text{ Jm}^2\text{V}^{-2}$, where a_0 denotes the Bohr radius and ϵ_0 is the vacuum permittivity. As can be seen from the obtained excitation resonances (Fig. 2(c)), the absolute lattice depth and thus the electric field amplitude is slightly different in the three directions. This difference is taken into account when determining the polarizabilities of the deeply bound molecules.

Figure 3 shows measured polarizabilities $\alpha^{(i)}$ of the molecules that we initially prepared in the rotational states $|0,0\rangle$ and $|2,0\rangle$ at a magnetic field of $B = 1000$ G. After production we adiabatically lower the magnetic field from $B = 1000$ G to 700 G, 400 G, and about 10 G. At each B -field we measure $\alpha^{(i)}$ in all three directions. As already seen in Fig. 2(a) the nonrotating state $|0,0\rangle$ (square plot symbols) exhibits an isotropic polarizability $\alpha^{(i)}$. This isotropy is reflected in the spherical symmetry of the rotational wavefunction for the molecular axis, $Y_{0,0}$, which is simply a constant. Correspondingly, the calculated expectation value $\langle A_i^2 \rangle$ is 1/3 for all directions. Thus, Eq. (1) simplifies to the useful relation $3\alpha^{(i)} = \alpha_{\parallel} + 2\alpha_{\perp}$.

Next, we study $\alpha^{(i)}$ for the state $|2,0\rangle$ down to $B = 400$ G (circles). As already observed in Fig. 2(b) there is a clear anisotropy of $\alpha^{(i)}$. The polarizabilities in the x - and y -

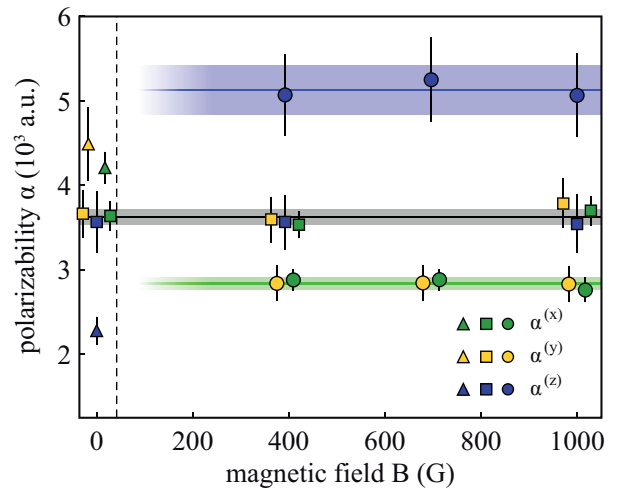


FIG. 3. (Color online). Polarizabilities $\alpha^{(i)}$, ($i = x, y, z$) of the Rb_2 triplet molecules for the rotational states $|R = 0, m_R = 0\rangle$ (squares), $|2,0\rangle$ (circles), and $|2,2\rangle$ (triangles) for different magnetic fields $B = 1000$ G, 700 G, 400 G, and about 10 G. The vertical line roughly indicates the magnetic field at which the quantum number m_R of the rotational state $R = 2$ changes (see text). For better visibility overlapping data points are shifted slightly with respect to each other in horizontal direction. The error bars are given by the uncertainty of the Lorentzian fits in the amplitude modulation spectra (cf. Fig. 2). For $|0,0\rangle$ and $|2,0\rangle$ the horizontal lines indicate the mean values of the measured polarizabilities with the shaded areas being the corresponding uncertainties.

directions are identical, but they differ from the one in the z -direction, which is the quantization axis. Using Eq. (1), we check for the consistency of the measurements using the fact that $\langle A_x^2 \rangle + \langle A_y^2 \rangle + \langle A_z^2 \rangle = 1$. The sum of the polarizabilities is then given by $\sum_i \alpha^{(i)} = \alpha_{\parallel} + 2\alpha_{\perp}$, which should be equal to $3\alpha^{(i)}$ of the state $|0,0\rangle$. Our experimental data fulfill this relation to within 1%. The fact that the polarizability $\alpha^{(i)}$ is independent of the magnetic field both for $|0,0\rangle$ and $|2,0\rangle$ highlights that the alignment of the molecular axis is not forced by the magnetic field B . The magnetic field only sets the direction of the quantization axis, stabilizing the spin polarization of the molecules.

We can use the measurements of $\alpha^{(i)}$ for state $|2,0\rangle = Y_{2,0}(\theta, \phi)$ to determine α_{\parallel} and α_{\perp} from Eq. (1). Using Eq. (2) we calculate $\langle A_x^2 \rangle = \langle A_y^2 \rangle = 0.2381$ and $\langle A_z^2 \rangle = 0.5238$ (cf. Fig. 1(b)). We obtain a set of two independent equations (the equations for the x - and y -directions are nominally identical) which can be uniquely solved, resulting in $\alpha_{\parallel} = 8.9(9) \times 10^3$ a.u. and $\alpha_{\perp} = 0.9(4) \times 10^3$ a.u. This large difference in the polarizability can be explained as mainly arising from the different lattice laser detuning with respect to the relevant electronic transitions. Due to selection rules for π - and σ -transitions, α_{\parallel} (α_{\perp}) is linked to $\Sigma - \Sigma$ ($\Sigma - \Pi$) transitions. As can be seen from Fig. 4, the detuning of our lattice laser from the Franck-Condon point on the $(1)^3\Pi_g$ potential curve is about 6 times larger than from that of the $(1)^3\Sigma_g^+$ potential

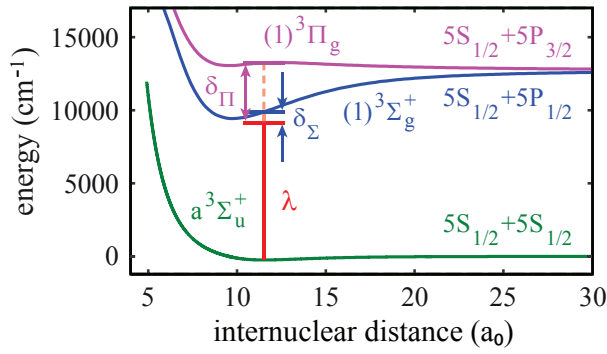


FIG. 4. (Color online). Detunings δ_Σ and δ_Π of the lattice laser at $\lambda = 1064.5$ nm from the two most relevant transitions, $a^3\Sigma_u^+ - (1)^3\Sigma_g^+$ and $a^3\Sigma_u^+ - (1)^3\Pi_g$, that determine the polarizabilities α_{\parallel} and α_{\perp} , respectively. The energy reference is given by the asymptote of the $a^3\Sigma_u^+$ potential. The potential curves are taken from [38].

curve, explaining the effect to good approximation.

We now look at the data points (triangles) at 10 G. Although these data are also obtained by preparing state $|2, 0\rangle$ and ramping down the B -field, they look quite different to the ones discussed previously. All polarizabilities change considerably and $\alpha^{(z)}$ is now smaller than $\alpha^{(x)}$ and $\alpha^{(y)}$. This indicates that the quantum state has changed, possibly due to an avoided crossing when sweeping the magnetic field. The sum rule $\sum_i \alpha^{(i)} = \alpha_{\parallel} + 2\alpha_{\perp}$ still holds, however. Since α_{\parallel} and α_{\perp} are known, we can directly extract the degrees of alignment from the measured polarizabilities $\alpha^{(i)}$ according to Eq. (1). From a common fit, using the constraints that $\langle A_x^2 \rangle = \langle A_y^2 \rangle$ and $\langle A_x^2 \rangle + \langle A_y^2 \rangle + \langle A_z^2 \rangle = 1$, we obtain $\langle A_{x,y}^2 \rangle = 0.42$ and $\langle A_z^2 \rangle = 0.16$. For magnetic fields below $B \sim 30$ G, coupled-channel calculations predict two quantum levels $|2, 2\rangle$ and $|2, 1\rangle$ (both with $m_F = 2, f = 2, I = 3, S = 1$) in the direct vicinity of the initial state $|2, 0\rangle$ [39]. Indeed, our measured values agree well with the calculated degrees of alignment ($\langle A_{x,y}^2 \rangle = 0.4286$ and $\langle A_z^2 \rangle = 0.1429$ of state $|2, 2\rangle$), whereas no agreement is found for $|2, 1\rangle$ ($\langle A_{x,y}^2 \rangle = 0.2857$ and $\langle A_z^2 \rangle = 0.4286$). We conclude that due to an avoided crossing the state $|2, 0\rangle$ turns into $|2, 2\rangle$ at low magnetic fields. Hence, the described method to probe the alignment of the molecular axis can also be used to gain information about the quantum numbers of rotational states and therefore has possible future applications in spectroscopy.

In conclusion, we have studied the alignment of ultracold nonpolar Rb_2 molecules in the $a^3\Sigma_u^+$ state with respect to all three spatial axes. Three states with different R and m_R quantum numbers were prepared in an optical lattice and investigated by measuring the dynamic polarizability via modulation spectroscopy. The rotational ground state $|0, 0\rangle$ shows an isotropic behavior, whereas the rotationally excited states $|2, 0\rangle$ and $|2, 2\rangle$ exhibit characteristic anisotropy. Furthermore, we determined the dynamic polarizabilities $\alpha_{\parallel} = 8.9(9) \times 10^3$ a.u. and $\alpha_{\perp} = 0.9(4) \times 10^3$ a.u. for the Rb_2 vibrational ground state of the $a^3\Sigma_u^+$ potential at a wavelength of 1064.5 nm. The present work paves the way for collisional

studies of aligned molecules in the triplet vibrational ground state and thus opens up new opportunities in the context of ultracold chemistry.

The authors would like to thank Eberhard Tiemann for providing results of coupled-channel calculations. We acknowledge Olivier Dulieu and Robert Moszyński for helpful discussions and information. This work was supported by the German Research Foundation (DFG). B.D. acknowledges support from the Carl-Zeiss-Stiftung.

- [1] H. Stapelfeldt and T. Seideman, *Rev. Mod. Phys.* **75**, 543 (2003).
- [2] M. Leshchko, R. V. Krems, J. M. Doyle, and S. Kais, *Molecular Physics* **111**, 1648 (2013).
- [3] R. N. Zare, *Science* **279**, 1875 (1998).
- [4] V. Aquilanti, M. Bartolomei, F. Pirani, D. Cappelletti, F. Vecchiocattivi, Y. Shimizu, and T. Kasai, *Phys. Chem. Chem. Phys.* **7**, 291 (2005).
- [5] Y. P. Chang, K. Długołęcki, J. Küpper, D. Rösch, D. Wild, and S. Willitsch, *Science* **342**, 6154, 98 (2013).
- [6] R. Neutze, R. Wouts, D. van der Spoel, E. Weckert, and J. Hajdu, *Nature* **406**, 752 (2000).
- [7] J. Itatani, J. Levesque, D. Zeidler, H. Niikura, H. Pépin, J. C. Kieffer, P. B. Corkum, and D. M. Villeneuve, *Nature* **432**, 867 (2004).
- [8] R. Torres, N. Kajumba, J. G. Underwood, J. S. Robinson, S. Baker, J. W. G. Tisch, R. de Nalda, W. A. Bryan, R. Velotta, C. Altucci, I. C. E. Turcu, and J. P. Marangos, *Phys. Rev. Lett.* **98**, 203007 (2007).
- [9] A. Barty, J. Küpper, and H. N. Chapman, *Annu. Rev. Phys. Chem.* **64**, 415 (2013).
- [10] M. Wu, R. J. Bemish, and R. E. Miller, *J. Chem. Phys.* **101**, 9447 (1994).
- [11] R. Baumfalk, N. H. Nahler, and U. Buck, *J. Chem. Phys.* **114**, 4755 (2001).
- [12] A. Gijsbertsen, W. Siu, M. F. Kling, P. Johnsson, P. Jansen, S. Stolte, and M. J. J. Vrakking, *Phys. Rev. Lett.* **99**, 213003 (2007).
- [13] I. Nevo, S. Kapishnikov, A. Birman, M. Dong, S. R. Cohen, K. Kjaer, F. Besenbacher, H. Stapelfeldt, T. Seideman, and L. Leiserowitz, *J. Chem. Phys.* **130**, 144704 (2009).
- [14] D. Shreenivas, A. Lee, N. Walter, D. Sampayo, S. Bennett, and T. Seideman, *J. Phys. Chem. A* **114**, 5674 (2010).
- [15] F. Krausz and M. Ivanov, *Rev. Mod. Phys.* **81**, 163 (2009).
- [16] P. B. Corkum, *Physics Today* **64**, 36 (2011).
- [17] N. F. Ramsey, *Phys. Rev.* **98**, 1853 (1955).
- [18] V. Aquilanti, D. Ascenzi, D. Cappelletti, and F. Pirani, *Nature* **371**, 399 (1994).
- [19] H. J. Loesch and A. Remscheid, *J. Chem. Phys.* **93**, 4779 (1990).
- [20] B. Friedrich and D. R. Herschbach, *Z. Phys. D* **18**, 153 (1991).
- [21] B. Friedrich and D. R. Herschbach, *Z. Phys. D* **24**, 25 (1992).
- [22] B. Friedrich and D. Herschbach, *Phys. Rev. Lett.* **74**, 4623 (1995).
- [23] S. M. Purcell and P. F. Barker, *Phys. Rev. Lett.* **103**, 153001 (2009).
- [24] L. Cai, J. Marango, and B. Friedrich, *Phys. Rev. Lett.* **86**, 775 (2001).
- [25] H. Sakai, S. Minemoto, H. Nanjo, H. Tanji, and T. Suzuki,

- Phys. Rev. Lett. **90**, 083001 (2003).
- [26] O. Ghafur, A. Rouzée, A. Gijbetsen, W. K. Siu, S. Stolte, and M. J. J. Vrakking, *Nat. Phys.* **5**, 289 (2009).
- [27] R. V. Krems, *Phys. Chem. Chem. Phys.* **10**, 4079 (2008).
- [28] M. H. G. de Miranda, A. Chotia, B. Neyenhuis, D. Wang, G. Quémener, S. Ospelkaus, J. L. Bohn, J. Ye, and D. S. Jin, *Nat. Phys.* **7**, 502 (2011).
- [29] B. Neyenhuis, B. Yan, S. A. Moses, J. P. Covey, A. Chotia, A. Petrov, S. Kotochigova, J. Ye, and D. S. Jin, *Phys. Rev. Lett.* **109**, 230403 (2012).
- [30] A. T. Krupp, A. Gaj, J. B. Balewski, P. Ilzhöfer, S. Hofferberth, R. Löw, and T. Pfau, M. Kurz, P. Schmelcher, arXiv 1401.4111 (2014).
- [31] C. Strauss, T. Takekoshi, F. Lang, K. Winkler, R. Grimm, and J. Hecker Denschlag, *Phys. Rev. A* **82**, 052514 (2010).
- [32] For a more general discussion without this simplification, see e.g. [40].
- [33] G. Thalhammer, K. Winkler, F. Lang, S. Schmid, R. Grimm, and J. Hecker Denschlag, *Phys. Rev. Lett.* **96**, 050402 (2006).
- [34] F. Lang, K. Winkler, C. Strauss, R. Grimm, and J. Hecker Denschlag, *Phys. Rev. Lett.* **101**, 133005 (2008).
- [35] J. Hecker Denschlag, H. Häffner, C. McKenzie, A. Browaeys, D. Cho, C. Helmerson, S. Rolston and W. D. Phillips, *J. Phys. B: At. Mol. Opt. Phys.* **35**, 3095 (2002).
- [36] J. G. Danzl, M. J. Mark, E. Haller, M. Gustavsson, R. Hart, J. Aldegunde, J. M. Hutson, and H.-C. Nägerl, *Nat. Phys.* **6**, 265 (2010).
- [37] M. S. Safronova, C. J. Williams, and C. W. Clark, *Phys. Rev. A* **69**, 022509 (2004).
- [38] J. Lozeille, A. Fioretti, C. Gabbanini, Y. Huang, H. K. Pechkis, D. Wang, P. L. Gould, E. E. Eyler, W. C. Stwalley, M. Aymar, and O. Dulieu, *Eur. Phys. J. D* **39**, 261 (2006).
- [39] E. Tiemann (private communication).
- [40] R. Vexiau, N. Bouloufa, M. Aymar, J. G. Danzl, M. J. Mark, H.-C. Nägerl, and O. Dulieu, *Eur. Phys. J. D* **65**, 243 (2011).